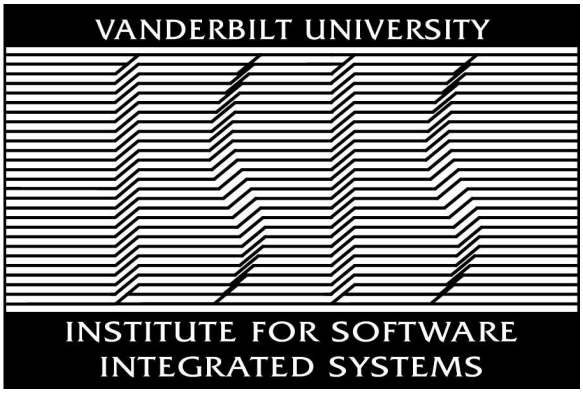

Institute for Software Integrated Systems
Vanderbilt University
Nashville, Tennessee, 37235

Constructive Non-Linear Control Design With Applications to Quad-Rotor and Fixed-Wing Aircraft

Nicholas Kottenstette

TECHNICAL REPORT

ISIS-10-101 Original: 1/2010

Constructive Non-Linear Control Design With Applications to Quad-Rotor and Fixed-Wing Aircraft

Nicholas Kottenstette*
*ISIS/Vanderbilt University

***Abstract*— This paper recalls a non-linear constructive method, based on controlling cascades of conic-systems as it applies to the control of quad-rotor aircraft. Such a method relied on the physical model of the system to construct high-performance, modest sampling period ($T_s = .02$ s) and low-complexity digital-controllers. The control of fixed-wing aircraft, however is not nearly a straight forward task in extending results related to the control of quad-rotor aircraft. Although fixed-wing aircraft and quad-rotor aircraft ultimately share the same kinematic equations of motion, fixed-wing aircraft are intimately dependent on their relationship to the wind reference frame. This additional coupling leads to additional equations of motion including those related to the angle-of-attack, slide-slip-angle, and bank angle. As a result a more advanced non-linear control method known as back-stepping is required to compensate for non-passive non-linearity's. These back-stepping controllers are recursive in nature and can even address actuator magnitude and rate limitations and even include adaptability to unknown lift and drag coefficients. This paper presents a non-adaptive back-stepping controller which is aimed to verify a fixed-wing aircraft model not subject to actuator limitations (in order to simplify discussion). The back-stepping controller proposed is less complex then previously proposed controllers, exhibits similar response characteristics while being robust to both steady head wind shear and discrete-time wind gust disturbances.**

I. INTRODUCTION

Quad-rotor helicopters are agile aircraft which are lifted and propelled by four rotors. Unlike traditional helicopters, they do not require a tail-rotor to control yaw and can use four smaller fixed-pitch rotors. Smaller rotors allow these vehicles to achieve higher velocities before blade flapping effects begin to introduce instability and limit performance. However, without an attitude control system it is difficult if not impossible for a human to successfully fly and maneuver such a vehicle. Thus, most research has focused on small unmanned aerial vehicles in which advanced embedded control systems could be developed to control these aircraft. In [1] a Lyapunov-like control approach is used to develop a non-linear inertial controller which relies on robust stability results involving control elements with nested saturation blocks [2], [3]. [4] shows that a simple, model-independent quaternion-based proportional derivative (PD) controller performs quite well in controlling attitude as compared to other more involved non-linear controllers. In [5], image based visual servo control algorithms are presented which exploit passivity-like properties of the dynamic model in order to derive Lyapunov control algorithms which rely on backstepping techniques. All the above papers, and others contain fairly detailed models which guide their overall control design.

[0]Contract/grant sponsor (number): NSF (NSF-CCF-0820088)
Contract/grant sponsor (number): Air Force (FA9550-06-1-0312).

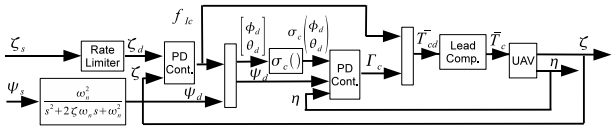

Fig. 1. Proposed quad-rotor control system [6].

As depicted in Fig. 1 we demonstrated how to use two PD controllers (denoted as PD Cont. in Fig. 1) to control the attitude and inertial position of a quad-rotor aircraft. The inner-most loop controller is a 'fast' PD attitude controller in which attitude is described by Euler angles η. The attitude controller design is initially justified by assuming that the controller and dynamics are passive. Next, we further assume that the resulting attitude controller is 'fast' enough that we can close the loop with a second PD inertial controller (the inertial position is denoted ζ). In order to compensate for the rotor-thrust lag effects, [7], an additional lead compensator was used to minimize this non-ideal effect (denoted as Lead Comp. in Fig. 1). Second, the rotors can only apply a fixed range of thrust (denoted $\sigma(\bar{T}_c)$ in which $\bar{T}_c$ denotes the corresponding thrust command vector) due to motor driver voltage limits. In order to address thrust actuator saturation [1] [2] we limited the range of attitude commands to our inner-loop PD controller in terms of pitch and roll to the interval $[-\frac{\pi}{4}, \frac{\pi}{4}]$ using the saturation function which is denoted as $\sigma_c()$ in Fig. 1. In addition, we chose to limit the maximum velocities by adding a position rate change limiter (depicted as 'Rate Limiter' in Fig. 1) to the desired inertial position set-point (denoted as ζ_s). The rate change limiter includes an additional second-order pre-filter applied to ζ_s in order to minimize overshoot. A similar filter is applied to the yaw set-point ψ_s as well.

In order to control fixed-wing aircraft the problem becomes quite more challenging. The fundamental difference between control of a quad-rotor aircraft and a fixed-wing aircraft is that the body forces for the fixed-wing aircraft are intimately dependent on the wind velocity vector. This dependence on the wind velocity vector, greatly complicates control design. In particular, the passivity-based arguments used to construct a high performance control law for a quad-rotor aircraft do not map over directly to the control of fixed-

wing aircraft. However, backstepping control techniques, which are closely related to passivity-based techniques, attempt to exploit much of the physical properties of a dynamic system by canceling out non-ideal affects in a very systematic manner to render the system to behave as a cascade of passive integrators with nested proportional feed-back loops [8]. Some of the recent literature which uses back-stepping control designs to control fixed-wing aircraft include the pioneering work in [9] which was systematically presented in [10] to tackle the generalized aircraft velocity-heading-angle-flight-path-angle control problem. One difficult problem in control of fixed-wing aircraft is getting a sufficient set of non-linear equations to describe the system, in which [10] provides one of the most complete accounts, which are recalled here (while clarifying some minor confusion relating drag-coefficients to body-forces).

The main contributions of this work include: i) a concise description of the key equations of motion in order to develop a sufficient model to simulate fixed wing aircraft, ii) a general non-linear backstepping control law (without adaptation, nor rate limitation) to quickly verify fixed-wing aircraft models and better understand and appreciate the more generalized result presented in [10], iii) a simple yet effective control strategy is presented for fixed-wing aircraft using only a small-angle assumption of the system description, which allows most of the key-equations of motion in tact but greatly simplifies the controller presented in [10] while maintaining close to the same range in performance, iv) an improved control law is proposed and verified to demonstrate excellent robustness to discrete-time wind gust disturbances.

Section II introduces the key kinematic equations of motion which are common to both a quad-rotor aircraft and a fixed-wing aircraft. Section III presents the remaining details in order to develop our model to simulate and control a fixed-wing aircraft. Section III also presents the simplified aerodynamic equations of motion which result from taking a small-angle assumption, and choosing to design the control law to keep the side-slip angle $\beta = 0$. Section IV presents how to determine the trim conditions of a fixed-wing aircraft in steady-state flight. Section V then introduces the reader to backstepping control techniques which includes Theorem 1 which is a generalized non-adaptive control law to achieve asymptotic stability and tracking of a set of desired trajectories applied to the most-outer control loop of triangular systems. Also in Section V we present a less complex control law in Theorem 2 which does not attempt to render a positive feed-back term $G(x)$ orthogonal and states that if the key feed-back gains are large-enough asymptotic stability can still be achieved. Section V-A presents an asymptotically stable control law which exploits back-stepping techniques and a classic passive control arrangement [6] to achieve near perfect tracking of the desired velocity trajectory $V_d(t)$. Section V-B presents the simplified back-stepping control law for the velocity flight-path and velocity heading angles. Section V-C presents the simplified back-stepping control law for the angle of attack, slide-slip, and bank-angle control. The simplified angular velocity control system is presented in Section V-D. Section VI presents detailed simulation results related to the control and verification of a Cessna A-37 Dragonfly, a United States Air Force light attack aircraft. The aircraft has to track aggressive test flight conditions as summarized in Section VI-A which achieves close tracking and robustness to a modified control law presented in Section VI-B which uses a filtered version of the additional feed-back term used in Theorem 1 to render orthogonal the effects of $G(x)$. Finally, conclusions are presented in Section VII.

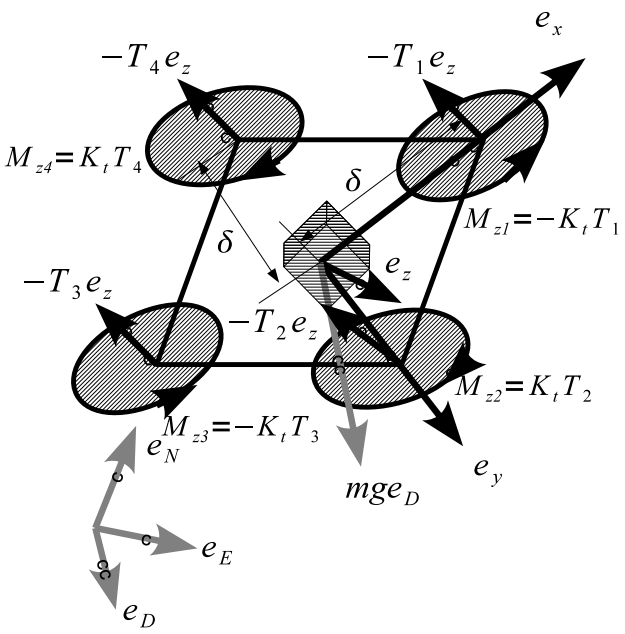

Fig. 2. UAV with depiction of inertial and body frames.

II. Quad-rotor Model

Let $\mathcal{I} = \{e_N, e_E, e_D\}$ (North-East-Down) denote the inertial frame, and $\mathcal{A} = \{e_x, e_y, e_z\}$ denote a frame rigidly attached to the aircraft as depicted in Fig. 2. Let ζ denote inertial position, η denote the vector of Euler angles $\eta^{\mathsf{T}} = \begin{bmatrix}\phi, & \theta, & \psi\end{bmatrix}^{\mathsf{T}}$ in which ϕ is the roll, θ is the pitch and ψ is the yaw. $R(\eta) \in \mathtt{SO}(3)$ is the orthogonal rotation matrix ($R^{\mathsf{T}}R = I$) which describes the orientation of the airframe in which $R(\eta)$ describes the rotation matrix from the inertial frame to the body frame as is the convention used in [11], [12]. The rotation matrix allows coordinates relative to the inertial frame such as inertial angular velocity ω_I to coordinates relative to the body frame such as the angular velocity ω as follows

$$\omega_I = R^{\mathsf{T}}(\eta)\omega.$$

In addition the time derivative of the rotation-matrix depends on the angular velocity as follows:

$$\dot{R}(\eta) = -(\omega\times)R(\eta)$$

In which $(\omega\times)$ is the cross-product which can be implemented using the following-skew-symmetric matrix

$(-(\omega\times) = (\omega\times)^\mathsf{T})$ operation:

$$\omega = [p,q,r]^\mathsf{T},\ (\omega\times) = \begin{bmatrix} 0 & -r & q \\ r & 0 & -p \\ -q & p & 0 \end{bmatrix}$$

The standard equations of motion are as follows:

$$\dot{\zeta} = v_I$$
$$m\dot{v_I} = f_I = mge_D + R^\mathsf{T}(\eta) f_b \quad (1)$$
$$I\dot{\omega} = -\omega \times I\omega + \Gamma \quad (2)$$
$$\dot{\eta} = J(\eta)\omega. \quad (3)$$

In which for a quad-rotor aircraft the body-force $f_b = -Te_z$. Which results in a cascade structure, where the inertial force (f_I) depends on the orientation as described by the Euler angle η. (3) relates the frame angular velocity ω to the rate change of the Euler angle $\dot{\eta}$ which depends on the frame control torque $\Gamma = [\gamma_x, \gamma_y, \gamma_z]^\mathsf{T}$. Each control torque is applied about each corresponding frame axis and positive torque follows the right hand rule. This cascade structure is an overall non-passive structure which has many passive elements. The overall approach in designing a controller for this system will be to take advantage of the passive elements to design a 'fast' passive attitude controller. The closed-loop dynamics of the attitude controller will be fast enough to ignore in order to implement a 'slower' passive inertial position controller which will command the desired attitude in order to reach a desired inertial position relative to the origin of the inertial frame ($\zeta = [X,Y,Z]^\mathsf{T}$). In the inertial frame, X is the relative distance from the origin along the e_E axis, Y is the relative distance from the origin along the e_N axis, and Z is the relative distance from the origin along the e_D axis. Note that $Z < 0, \dot{Z} < 0$ corresponds to the UAV above the inertial origin and flying upward.

Using the shorthand notation $c_x = \cos x$ and $s_x = \sin x$, the rotation matrix $R(\eta)$ is related to the Euler angles as follows [11, Section 5.6.2]:

$$R(\eta) = \begin{bmatrix} c_\theta c_\psi & c_\theta s_\psi & -s_\theta \\ s_\phi s_\theta c_\psi - c_\phi s_\psi & s_\phi s_\theta s_\psi + c_\phi c_\psi & c_\theta s_\phi \\ c_\phi s_\theta c_\psi + s_\phi s_\psi & c_\phi s_\theta s_\psi - s_\phi c_\psi & c_\theta c_\phi. \end{bmatrix} \quad (4)$$

The matrix $J(\eta)$ is the inverse of the Euler angle rates matrix $[E'_{123}(\eta)]^{-1}$ [11, Section 5.6.4] such that

$$J(\eta) = \begin{bmatrix} 1 & \sin\phi\tan\theta & \cos\phi\tan\theta \\ 0 & \cos\phi & -\sin\phi \\ 0 & \frac{\sin\phi}{\cos\theta} & \frac{\cos\phi}{\cos\theta} \end{bmatrix}. \quad (5)$$

III. Fixed-Wing Aircraft Model

The equations of motion for a fixed-wing aircraft are identical as those given for a quad-rotor aircraft. The fundamental difference is that the body-forces f_b and the control-torques Γ are intimately dependent on engine-thrust, and the velocity-reference-frame. The body-force f_b is typically determined from the aircraft-stability forces $f_s = [f_{sx}, f_{sy}, f_{sz}]^\mathsf{T}$ which depend on the dynamic-pressure $\bar{q} = \frac{1}{2}\rho V^2$ (ρ density of air, $V = \sqrt{v_I^\mathsf{T} v_I} = \sqrt{v_b^\mathsf{T} v_b}$, $v_b = R(\eta)v_I$), the aircraft's reference area S and the respective drag (C_{Ds}), side-force (C_Y) and lift (C_L) coefficients (with respect to the stability axis) such that

$$f_s = \bar{q}S[-C_{Ds}, C_Y, -C_L]^\mathsf{T}$$
$$f_b = R_{\mathsf{b/s}}(\alpha) f_s$$
$$f_b = \bar{q}S \begin{bmatrix} \cos(\alpha) & 0 & -\sin(\alpha) \\ 0 & 1 & 0 \\ \sin(\alpha) & 0 & \cos\alpha \end{bmatrix} \begin{bmatrix} -C_{Ds} \\ C_Y \\ -C_L \end{bmatrix}.$$

In which α is the angle-of-attack [13]. The angle-of-attack α and side-slip angle β, unlike pitch θ and yaw ψ, do not relate the orientation of the body-frame to the inertial-frame but depend on non-linear ratios of the body-velocities $v_b = [u,v,w]^\mathsf{T}$.

$$\alpha = \tan^{-1}\frac{w}{u},\ \dot{\alpha} = \frac{u\dot{w} - w\dot{u}}{u^2 + w^2}$$
$$\beta = \sin^{-1}\frac{v}{V},\ \dot{\beta} = \frac{V\dot{v} + v\dot{V}}{V^2\cos\beta}.$$

Note, that for simplicity of discussion we shall assume the wind-velocity v_w relative to the inertial frame is considered zero. However, it is noted that all aerodynamic drag and lift effects are captured in simulation by taking $v_{b_a} = R(\eta)(v_I - v_w)$, determining the corresponding aerodynamic-forces and applying them to the equations of motion. For simulation we assume the stability-drag-coefficients depend on α, β, aileron angle δ_a, fixed-incidence angle δ_f, elevator angle δ_e, and rudder angle δ_e as follows:

$$\begin{bmatrix} C_{Ds} \\ C_Y \\ C_L \end{bmatrix} = \begin{bmatrix} C_{D\alpha}\alpha \\ C_{Y\beta}\beta \\ C_{L\alpha}\alpha \end{bmatrix} + \begin{bmatrix} C_{Do} + C_{D\mathsf{in}}\delta_f \\ C_{Yo} \\ C_{Lo} + C_{L\mathsf{in}}\delta_f \end{bmatrix} + \frac{1}{2V}\begin{bmatrix} 0 & C_{Dq}\bar{c} & 0 \\ C_{Yp}b & 0 & C_{Yr}b \\ 0 & C_{Lq}\bar{c} & 0 \end{bmatrix}\begin{bmatrix} p \\ q \\ r \end{bmatrix} + \begin{bmatrix} C_{D\delta_e} & 0 & 0 \\ 0 & C_{Y\delta_a} & C_{Y\delta_r} \\ C_{L\delta_e} & 0 & 0 \end{bmatrix}\begin{bmatrix} \delta_e \\ \delta_a \\ \delta_r \end{bmatrix}$$

in which b is the wing-span and $\bar{c}$ is the mean aerodynamic chord. In a similar manner, the body torques are determined as follows $\Gamma = \bar{q}S[bC_l,\ \bar{c}C_m,\ bC_n]^\mathsf{T}$:

$$\begin{bmatrix} C_l \\ C_m \\ C_n \end{bmatrix} = \begin{bmatrix} C_{l\beta}\beta \\ C_{m\alpha}\alpha \\ C_{n\beta}\beta \end{bmatrix} + \begin{bmatrix} C_{lo} \\ C_{mo} + C_{m\mathsf{in}}\delta_f \\ C_{no} \end{bmatrix} + \frac{1}{2V}\begin{bmatrix} C_{lp}b & 0 & C_{lr}b \\ 0 & C_{mq}\bar{c} & 0 \\ C_{np}b & 0 & C_{nr}b \end{bmatrix}\begin{bmatrix} p \\ q \\ r \end{bmatrix} + \begin{bmatrix} 0 & C_{l\delta_a} & C_{l\delta_r} \\ C_{m\delta_e} & 0 & 0 \\ 0 & C_{n\delta_a} & C_{n\delta_r} \end{bmatrix}\begin{bmatrix} \delta_e \\ \delta_a \\ \delta_r \end{bmatrix}$$

It will be helpful to use the more compact notation:

$$\Gamma = \bar{q}S\,\mathrm{diag}(b,\bar{c},b)\left[C_{\Gamma(\alpha,\beta)} + C_{\Gamma o} + \frac{1}{2V}C_{\Gamma\omega}\omega + C_{\Gamma\delta}\delta\right]$$

in which $\delta = [\delta_e, \delta_a, \delta_r]^\mathsf{T}$. Typically, the matrix $C_{\Gamma\omega}$ has the stabilizing property of being negative-definite, and can be

easily verified using the Sylvester criteria:

$$\begin{gathered} C_{\Gamma\omega} \text{ is negative-definite if and only if} \\ C_{lp}, C_{mq}, C_{nr} < 0 \quad \text{and} \\ (C_{np} + C_{lr})^2 < 4 C_{lp} C_{nr}. \end{gathered}$$

The torque applied to the fixed-wing aircraft has three components, a disturbance component Γ_{d}, a stabilizing component Γ_ω and an actuator component Γ_δ in which:

$$\begin{aligned} \Gamma &= \Gamma_{\mathsf{d}} + \Gamma_\omega + \Gamma_\delta \\ \Gamma_{\mathsf{d}} &= \bar{q} S \,\mathrm{diag}(b, \bar{c}, b)[C_{\Gamma(\alpha,\beta)} + C_{\Gamma o}] \\ \Gamma_\omega &= \frac{\rho(h) V S}{4} \,\mathrm{diag}(b, \bar{c}, b) C_{\Gamma\omega} \omega \\ \Gamma_\delta &= \bar{q} S \,\mathrm{diag}(b, \bar{c}, b) C_{\Gamma\delta} \delta \end{aligned}$$

Finally, the inertia for most fixed-wing aircraft, due to their symmetry of their bodies along the x-axis in the x-y-plain implies that $I_{xy} = 0$ and their symmetry along the z-axis in the y-z-plain implies $I_{yz} = 0$. Therefore, the inertia-matrix has the following general form:

$$I = \begin{bmatrix} I_{xx} & 0 & -I_{xz} \\ 0 & I_{yy} & 0 \\ -I_{xz} & 0 & I_{zz} \end{bmatrix}$$

in which $I_{xx}, I_{yy}, I_{zz}, -I_{xz} > 0$. These equations are sufficient to develop a fairly complete simulation of the dynamics related to fixed-wing aircraft [14] and the respective coefficients can be obtained from the UIUC Applied Aerodynamics Group web site [15].

Gravitational dependency on altitude $h = |Z|$ are modelled as follows:

$$g(h) = g_o \left(\frac{R}{R+h} \right)^2$$

in which $R = 6356 \times 10^3$ meters is the radius of the earth and $g_o = 9.80665\ m/s^2$. In addition air-density $\rho(h)$ and speed of sound $a(h)$ is computed as follows:

$$\begin{aligned} T(h) &= T_o - L \times h \times 10^{-3} \\ P_s(h) &= P_o \left(\frac{T(h)}{T_o} \right)^{\frac{M \times g(h)}{R \times L}} \\ \rho(h) &= \frac{P_s(h)}{\frac{1000 \times R}{M} \times T(h)} \\ a(h) &= \sqrt{\gamma \times \frac{1000 \times R}{M} \times T(h)} \end{aligned}$$

in which $R = 8.31432$ J/(mol-Kelvin), $M = 28.9644$ gm/mol, $T_o = 288.15$ Kelvin (standard temperature), $P_o = 101325$ Pascals (standard pressure), $L = 6.5$ Kelvin/km, $\gamma = 1.4$ gas-constant for air.

Most fixed-wing aircraft controllers focus on maintaining a desired velocity V and appropriate angle of attack α in order to maintain a given altitude. In addition, in order to achieve a desired heading they focus on controlling a given bank-angle (μ) relative to the velocity vector which should not be confused with the attitude roll angle (ϕ). As a result, the following equations of motion are used to guide controller design:

$$m\dot{V} = F_T \cos(\alpha)\cos(\beta) - D + mg_1 \tag{6}$$

$$mV\dot{\beta} = -F_T \cos(\alpha)\sin(\beta) - C + mg_2 - mVr_s \tag{7}$$

$$\begin{aligned} mV\cos(\beta)\dot{\alpha} = &- F_T \sin(\alpha) - L + mg_3 \\ &+ mV\left(q\cos(\beta) - p_s \sin(\beta)\right) \end{aligned} \tag{8}$$

In which $\omega_s = [p_s, q_s, r_s]^{\mathsf{T}}$ are the body angular velocities with respect to the stability axis $\omega_s = R^{\mathsf{T}}_{\mathsf{b/s}} \omega$:

$$\begin{bmatrix} p_s \\ q \\ r_s \end{bmatrix} = \begin{bmatrix} \cos(\alpha) & 0 & \sin(\alpha) \\ 0 & 1 & 0 \\ -\sin(\alpha) & 0 & \cos(\alpha) \end{bmatrix} \begin{bmatrix} p \\ q \\ r \end{bmatrix}.$$

$-D, -C, -L$ are the respective forces with respect to the wind-axis in which $f_w = [-D, -C, -L]^{\mathsf{T}}$ and are related to the stability force vector f_s as follows ($f_w = R_{\mathsf{w/s}} f_s$):

$$\begin{bmatrix} -D \\ -C \\ -L \end{bmatrix} = \bar{q} S \begin{bmatrix} \cos(\beta) & \sin(\beta) & 0 \\ -\sin(\beta) & \cos(\beta) & 0 \\ 0 & 0 & 1 \end{bmatrix} \begin{bmatrix} -C_{D_s} \\ C_Y \\ -C_L \end{bmatrix}.$$

The effective gravity terms g_1, g_2, g_3 depend on attitude, α and β as follows:

$$\begin{aligned} g_1 &= g(h)\left[-c_\alpha c_\beta s_\theta + (s_\beta s_\phi + s_\alpha c_\beta c_\phi) c_\theta\right] \\ g_2 &= g(h)\left[c_\theta s_\phi c_\beta + (c_\alpha s_\theta - s_\alpha c_\theta c_\phi) s_\beta\right] \\ g_3 &= g(h)\left(c_\alpha c_\theta c_\phi + s_\alpha s_\theta\right). \end{aligned}$$

If we introduce two additional terms: velocity flight-path angle γ and velocity heading angle χ (from the north) in which

$$\begin{aligned} -\gamma &= \sin^{-1}\left(\frac{v_{I3}}{V}\right) \\ &= \sin^{-1}\left[-c_\alpha c_\beta s_\theta + (s_\beta s_\phi + s_\alpha c_\beta c_\phi) c_\theta\right] \end{aligned}$$

and

$$\begin{aligned} \chi &= \cos^{-1}\left[\frac{v_{I1}}{\sqrt{v_{I1}^2 + v_{I2}^2}}\right] \\ &= \sin^{-1}\left[\frac{v_{I2}}{\sqrt{v_{I1}^2 + v_{I2}^2}}\right] \end{aligned}$$

Finally, noting that the bank-angle has the following relationships:

$$\begin{aligned} \mu &= \sin^{-1}\left\{\frac{\left[c_\theta s_\phi c_\beta + (c_\alpha s_\theta - s_\alpha c_\theta c_\phi) s_\beta\right]}{\cos\gamma}\right\} \\ &= \cos^{-1}\left\{\frac{\left(c_\alpha c_\theta c_\phi + s_\alpha s_\theta\right)}{\cos\gamma}\right\} \end{aligned}$$

then the expressions for the effective gravity terms can be written in the following compact form:

$$\begin{aligned} g_1 &= -g(h)\sin(\gamma) \\ g_2 &= g(h)\sin(\mu)\cos(\gamma) \\ g_3 &= g(h)\cos(\mu)\cos(\gamma). \end{aligned}$$

Finally, we recall the equations of motion for $\dot{\gamma}$, $\dot{\chi}$, and $\dot{\mu}$ [10], [13], [14], [16]:

$$\begin{aligned}\dot{\gamma} =& -\frac{g}{V}\cos(\gamma) + \frac{1}{mV}[C\sin(\mu) + L\cos(\mu) \\ &+ F_T(\sin(\alpha)\cos(\mu) + \cos(\alpha)\sin(\beta)\sin(\mu))]\end{aligned} \tag{9}$$

$$\begin{aligned}\dot{\chi} =& \frac{1}{mV}[-C\cos(\mu) + L\sin(\mu) \\ &+ F_T(\sin(\alpha)\sin(\mu) - \cos(\alpha)\sin(\beta)\cos(\mu))]\end{aligned} \tag{10}$$

$$\begin{aligned}\dot{\mu} =& \frac{1}{mV}[-C\tan(\gamma)\cos(\mu) + L(\tan(\beta) + \tan(\gamma)\sin(\mu)) \\ &+ F_T(\sin(\alpha)\sin(\mu)\tan(\gamma) + \sin(\alpha)\tan(\beta) \\ &- \cos(\alpha)\sin(\beta)\cos(\mu)\tan(\gamma))] \\ &- \frac{g}{V}\tan(\beta)\cos(\gamma)\cos(\mu) + \frac{p_s}{\cos(\beta)}\end{aligned} \tag{11}$$

Our primary goal is to provide a flight-control system which allows a group of aircraft to hold a formation in order to refuel in a quick and efficient manner. We shall take a two-pronged approach in developing a formation control system by developing an inertial navigation controller for each plane and couple it to an outer-loop controller to maintain the formation. The focus of this paper will be to develop an appropriate inertial navigation controller. Most successful formation control papers neglect the effects of β because an inner-loop controller keeps $\beta = 0$ [14], [16]. As shown in [9] β can be effectively controlled using a non-linear back-stepping controller which determines the respective body-angular-velocity about the stability z-axis r_s. Likewise a similar controller can be designed to control α which determines the respective body-angular-velocity about the stability y-axis $q = q_s$. Finally, it should be readily evident that a similar controller can be designed to control μ which determines the respective body-angular-velocity about the stability x-axis p_s. Without much loss of generality we can assume that α, γ are small and for the β controller, β is small. This allows us to greatly simplify the equations of motion, reduce computational complexity, and still capture most of the non-linear dynamics for flight control.

$$m\dot{V} = F_T - \bar{q}S(C_{Do} + C_{D\mathsf{in}}\delta_f) + \Delta f_V(x) \tag{12}$$

$$\Delta f_V(x) = -\bar{q}S\left[C_{D\alpha}\alpha + \left(\frac{C_{Dq}\bar{c}}{2V}\right)q + C_{D\delta_e}\delta_e\right] - mg(h)\gamma$$

$$m\dot{\gamma} = -\frac{1}{V}[mg + \bar{q}S(C_Y\sin(\mu) - C_L\cos(\mu)) - F_T\cos(\mu)\alpha]$$

$$m\dot{\gamma} = \left(0.5\rho(h)VSC_{L\alpha} + \frac{F_T}{V}\right)\cos(\mu)\alpha + \Delta f_\gamma(x) \tag{13}$$

$$\Delta f_\gamma(x) = -\frac{1}{V}\left[mg + \bar{q}S(C_Y\sin(\mu) - C_L(x)\cos(\mu))\right]$$

$$C_L(x) = C_{Lo} + C_{L\mathsf{in}}\delta_f + \left(\frac{C_{Lq}\bar{c}}{2V}\right)q + C_{L\delta_e}\delta_e$$

$$\dot{\chi} = \frac{1}{mV}[\bar{q}S(C_Y\cos(\mu) + C_L\sin(\mu)) + F_T\sin(\mu)\alpha]$$

$$\dot{\chi} = \cos(\mu)\left\{\frac{1}{mV}[\bar{q}SC_L + F_T\alpha]\tan(\mu) + \frac{\bar{q}SC_Y}{mV}\right\} \tag{14}$$

$$\dot{\alpha} = -\frac{F_T + \bar{q}SC_{L\alpha}}{mV}\alpha + \left(1 - \frac{\rho(h)C_{Lq}\bar{c}}{4m}\right)q + \Delta f_\alpha(x) \tag{15}$$

$$\begin{aligned}\Delta f_\alpha(x) =& -\frac{1}{mV}[\bar{q}S(C_{Lo} + C_{L\mathsf{in}}\delta_f + C_{L\delta_e}\delta_e) \\ &- mg(h)\cos(\mu)]\end{aligned}$$

$$\dot{\mu} = p + \alpha r + \Delta f_\mu(x) \tag{16}$$

$$\begin{aligned}\Delta f_\mu(x) =& \frac{\gamma}{mV}[\bar{q}S(C_Y\cos(\mu) + C_L\sin(\mu)) \\ &+ F_T\alpha\sin(\mu)]\end{aligned}$$

$$\begin{aligned}\dot{\beta} =& -\frac{F_T - \bar{q}S(C_{Y\beta} + C_{Ds})}{mV}\beta + (-1 + \frac{b\rho(h)C_{Yr}}{4m})r \\ &+ (\alpha + \frac{b\rho(h)C_{Yp}}{4m})p + \Delta f_\beta(x)\end{aligned} \tag{17}$$

$$\begin{aligned}\Delta f_\beta(x) =& \frac{1}{mV}[\bar{q}S(C_{Yo} + C_{Y\delta_a}\delta_a + C_{Y\delta_r}\delta_r) \\ &+ mg(h)\sin(\mu)]\end{aligned}$$

$$I\dot{\omega} = -\omega \times I\omega + \Gamma_c \tag{18}$$

$$\Gamma_c = \Gamma_\omega + \Gamma_{\mathsf{d}} + \Gamma_\delta.$$

IV. Fixed-Wing Aircraft Trim Conditions

In order to determine the appropriate thrust, angle-of-attack, etc. for our initial simulation parameters we do the following:

1. Given: V, h
2. Assume: $\gamma = \chi = \beta = \mu = \dot{\gamma} = \dot{\chi} = \dot{\alpha} = \dot{\beta} = \dot{\mu} = \dot{V} = 0$, in addition C_{Yo} is typically zero, therefore $p = r = \delta_a = \delta_r = 0$ and since α is small assume $\cos(\alpha) = 1$, $\sin(\alpha) = \alpha$, finally we assume $C_{lo} = C_{no} = 0$ (typical).
3. Observe, from (8) and (9) imply that $q = 0$ and that our assumptions imply that $\Gamma_{\mathsf{d}} + \Gamma_\omega + \Gamma_\delta = 0$.
4. Solve for $F_T,\ \alpha,\ \delta_e$ from the following equations:

$$\begin{aligned}F_T - \bar{q}S\left(C_{D\alpha}\alpha + C_{D\delta_e}\delta_e\right) &= \bar{q}S\left(C_{Do} + C_{D\mathsf{in}}\delta_f\right) \\ F_T\alpha + \bar{q}S\left(C_{L\alpha}\alpha + C_{L\delta_e}\delta_e\right) &= -\bar{q}S\left(C_{Lo} + C_{L\mathsf{in}}\delta_f\right) \\ &\quad + mg(h) \\ C_{m\delta_e}\delta_e + C_{m\alpha}\alpha &= -C_{mo} - C_{m\mathsf{in}}\delta_f\end{aligned}$$

V. Control System Design

Backstepping control techniques pioneered by [9] and systematically formalized by [10] provide a systematic manner to quickly get a working non-linear control system based on the physical model of the aircraft. Therefore if the aircraft model is correctly implemented and the control design, based on the physical model of the aircraft is implemented correctly a stable aircraft velocity V, flight-path angle γ, and heading-angle χ will be created. Since we have a fairly accurate model of a fixed-wing aircraft, adaptation is not necessary. Therefore we wish to implement a simplified back-stepping controller similar to the controller presented in [17, Theorem 1] [10, Theorem 2] (except that we do not use adaptation nor do we consider actuator limitations in order to simplify discussion) which can be applied to our fixed-wing aircraft model in order to verify that the model is correct. In fact the following control law can be

applied systematically to any non-linear system which can be realized in the following triangular form.

Assumption 1: Assume that we have a non-linear system Σ with m n-dimensional state vectors $F_j(x),\ x_j\ \in \mathbb{R}^n\ j\ \in \{1,\ldots,m\}\ x = [x_1^\mathsf{T},\ldots,x_m^\mathsf{T}]^\mathsf{T}$ which can be described by the following triangular set of ordinary differential equations:

$$\begin{aligned}\dot{x}_1 =& F_1(x) + G_1(x)x_2\\ \dot{x}_2 =& F_2(x) + G_2(x)x_3\\ \vdots =& \ \vdots\\ \dot{x}_{m-1} =& F_{m-1}(x) + G_{m-1}(x)x_m\\ \dot{x}_m =& F_m(x) + G_m(x)u.\end{aligned}$$

In addition it is assumed that $F_j(x)$ is known and the inverse for $G_j(x)$ (denoted $G_j^{-1}(x)$) exists for all j and x.

Theorem 1: Denote the difference between the desired state-trajectory $x_{j\mathsf{d}}$ and actual state x_j as $\hat{x}_j = (x_j - x_{j\mathsf{d}})$. The non-linear system Σ described by Assumption 1 with the following controller $k_1,\ldots,k_m > 0$:

$$\begin{aligned}u =& G_m^{-1}(x)(-F_m(x) - k_m\hat{x}_m + \dot{x}_{m\mathsf{d}}\\ &- G_{m-1}^\mathsf{T}(x)\hat{x}_{m-1})\\ x_{m\mathsf{d}} =& G_{m-1}^{-1}(x)(-F_{m-1}(x) - k_{m-1}\hat{x}_{m-1} + \dot{x}_{(m-1)\mathsf{d}}\\ &- G_{m-2}^\mathsf{T}(x)\hat{x}_{m-2})\\ \vdots =& \ \vdots\\ x_{3\mathsf{d}} =& G_2^{-1}(x)\left(-F_2(x) - k_2\hat{x}_2 + \dot{x}_{2\mathsf{d}} - G_1^\mathsf{T}(x)\hat{x}_1\right)\\ x_{2\mathsf{d}} =& G_1^{-1}(x)\left(-F_1(x) - k_1\hat{x}_1 + \dot{x}_{1\mathsf{d}}\right)\end{aligned}$$

is globally asymptotically stable such that $\lim_{t\to\infty}\hat{x}_j(t) = 0$.

Proof: First we observe that by applying the proposed control law we can described the error dynamics in the following compact form (in which $\hat{x} = [\hat{x_1}^\mathsf{T},\ldots,\hat{x}_m^\mathsf{T}]^\mathsf{T}$):

$$\begin{aligned}\dot{\hat{x}} =& -\operatorname{diag}\{k_1,\ldots,k_m\}\hat{x} + \bar{G}(x)\hat{x}\\ \bar{G}(x) =& G(x) - G^\mathsf{T}(x)\\ G(x) =& \begin{bmatrix}0 & \operatorname{diag}\{G_1(x),G_2(x),\ldots,G_{m-1}(x)\}\\ 0 & 0\end{bmatrix}\end{aligned}$$

We note that the matrix $\bar{G}(x)$ has the important property that it is skew symmetric ($\bar{G}(x) = -\bar{G}^\mathsf{T}(x)$) therefore if we choose the following Lyapunov function $V_L(\hat{x})$ such that

$$V_L(\hat{x}) = \frac{1}{2}\hat{x}^\mathsf{T}\hat{x} > 0$$

in which the derivative is easily computed to be:

$$\begin{aligned}\dot{V}_L(\hat{x}) =& \hat{x}^\mathsf{T}\left(-\operatorname{diag}\{k_1,\ldots,k_m\} + \bar{G}(x)\right)\hat{x}\\ =& -\hat{x}^\mathsf{T}\operatorname{diag}\{k_1,\ldots,k_m\}\hat{x} < 0\end{aligned}$$

for all $\hat{x} \neq 0$ when $k_j > 0$. The final inequality is a direct result of the skew-symmetry property of $\bar{G}(x)$. ■

We observe that although this result is quite general, it is typically not necessary to introduce the additional feed-back term $-G^\mathsf{T}(x)$ in order to fully-cancel the effects of $G(x)$ in order to render $\dot{V}_L(\hat{x})$ negative definite. For the special case when all the feed-back gains $k_j\ \in \mathbb{R}$ are large enough and the eigenvalues for $G(x)$ are bounded then the previously mentioned Lyapunov function can be rendered negative definite.

Theorem 2: Denote the difference between the desired state-trajectory $x_{j\mathsf{d}}$ and actual state x_j as $\hat{x}_j = (x_j - x_{j\mathsf{d}})$ in addition let $\lambda_{\max}(G^\mathsf{T}(x) + G(x))$ denote the maximum eigenvalue of the matrix $(G^\mathsf{T}(x) + G(x))$ in which

$$G(x) = \begin{bmatrix}0 & \operatorname{diag}\{G_1(x),G_2(x),\ldots,G_{m-1}(x)\}\\ 0 & 0\end{bmatrix}.$$

The non-linear system Σ described by Assumption 1 with real scalar control gains $k_1,\ldots,k_m > 0$ in which the minimum real gain $k_{\min} > \frac{1}{2}\lambda_{\max}(G^\mathsf{T}(x) + G(x))$ and implements the following control law:

$$\begin{aligned}u =& G_m^{-1}(x)(-F_m(x) - k_m\hat{x}_m + \dot{x}_{m\mathsf{d}})\\ x_{m\mathsf{d}} =& G_{m-1}^{-1}(x)(-F_{m-1}(x) - k_{m-1}\hat{x}_{m-1} + \dot{x}_{(m-1)\mathsf{d}})\\ \vdots =& \ \vdots\\ x_{3\mathsf{d}} =& G_2^{-1}(x)\left(-F_2(x) - k_2\hat{x}_2 + \dot{x}_{2\mathsf{d}}\right)\\ x_{2\mathsf{d}} =& G_1^{-1}(x)\left(-F_1(x) - k_1\hat{x}_1 + \dot{x}_{1\mathsf{d}}\right)\end{aligned}$$

is globally asymptotically stable such that $\lim_{t\to\infty}\hat{x}_j(t) = 0$.

Proof: First we observe that by applying the proposed control law we can described the error dynamics in the following compact form (in which $\hat{x} = [\hat{x_1}^\mathsf{T},\ldots,\hat{x}_m^\mathsf{T}]^\mathsf{T}$):

$$\dot{\hat{x}} = -\operatorname{diag}\{k_1,\ldots,k_m\}\hat{x} + G(x)\hat{x}$$

Again we choose the following Lyapunov function $V_L(\hat{x})$ such that

$$V_L(\hat{x}) = \frac{1}{2}\hat{x}^\mathsf{T}\hat{x} > 0$$

in which the derivative is easily computed to be:

$$\dot{V}_L(\hat{x}) = \hat{x}^\mathsf{T}\left(-\operatorname{diag}\{k_1 I,\ldots,k_m I\} + G(x)\right)\hat{x}$$

which is negative-definite for all $\hat{x} \neq 0$ when $k_{\min} > \lambda_{\max}(G^\mathsf{T}(x) + G(x))$. The following property holds because we observe that the matrix:

$$-\operatorname{diag}\{k_1 I,\ldots,k_m I\} + G(x) \text{ is negative definite iff}$$

$$\text{the eigenvalues of } \frac{1}{2}(-2\operatorname{diag}\{k_1 I,\ldots,k_m I\} + G^\mathsf{T} + G)$$

$$\text{are negative.}$$

$$-\operatorname{diag}\{k_1 I,\ldots,k_m I\} + \frac{1}{2}(G^\mathsf{T} + G) =$$

$$-\operatorname{diag}\{k_1 I,\ldots,k_m I\} + \frac{1}{2}P\Lambda_{G^\mathsf{T}+G}P^{-1})$$

$$\text{in which the eigenvalues are as follows}$$

$$-\operatorname{diag}\{k_1 I,\ldots,k_m I\} + \frac{1}{2}\Lambda_{G^\mathsf{T}+G}.$$

Which are clearly negative if $k_{\min} > \lambda_{\max}(G^\mathsf{T}(x) + G(x))$. ■

We also observe that the resulting controller dynamics are such that $\hat{x}_m$ converges to zero asymptotically as long as $k_m > 0$, and the remaining error terms depend only on the cascaded error input preceding them with a strictly-output

error dynamics which result from their respective negative-error-state-feedback loop. Therefore as long as the maximum singular-value of $G(x)$ is bounded, the error outputs will be bounded as well. We will test our control-system with and without this additional feed-back term which includes $G(x)$. In general we get better tracking of γ_{d} and χ_{d} when $G(x)$ is introduced, however, when discrete-time wind gusts are introduced the control system which does not include $G(x)$ in the feed-back term appears to more gracefully handle such a disturbance.

A. Velocity Control

From (12) it is readily apparent that velocity control system can be implemented by determining an appropriate thrust command in order to maintain V therefore we propose the following control system. All controllers will be implemented as discrete-time controllers at a sampling period T_s. In order to preserve conic-properties of our discrete-time controllers, we will use the *IPESH*-Transform for synthesis [18], [19]. Using the following back-stepping control law (19),

$$F_T = \bar{q}S(C_{\mathsf{Do}} + C_{\mathsf{Din}}\delta_f) - \Delta f_V(x) - m\omega_c V(t) + F_{Tc}(t). \tag{19}$$

the dynamics involving the velocity of the fixed-wing aircraft are as follows

$$\dot{V}(t) = -\omega_c V(t) + \frac{F_{Tc}(t)}{m}$$

which results in a strictly-output-passive system. Therefore, the following steady-state tracking and strictly-positive-real controller ($k_V > 0$) in terms of the Laplace-Transforms complex argument s and desired velocity reference $V_{\mathsf{d}}(t)$ can be used to compute $F_{Tc}(t)$

$$\frac{F_{Tc}(s)}{V_{\mathsf{d}}(s) - V(s)} = mk_V\frac{s+\omega_c}{s}.$$

The resulting strictly-output-passive system dynamics show that the system will track $V_{\mathsf{d}}(t)$ at steady-state while remaining asymptotically-stable

$$\dot{V}(t) = -k_V V(t) + k_V V_{\mathsf{d}}(t).$$

B. Flight-Path and Velocity Heading Angle Control

Let $x_1 = [\chi, \gamma]^{\mathsf{T}}$, further approximating $\cos(\mu) = 1$ and $\sin(\mu) = \mu$ we further simplify (14) and (13) in order to assume the following model for $\dot{x}_1$

$$\begin{gathered}\dot{x}_1 = F_1(x) + G_1(x)x_{2\mathsf{s}}\\ F_1(x) = [\frac{\bar{q}SC_Y}{mV},\ \frac{\Delta f_\gamma(x)}{m}]^{\mathsf{T}}\\ G_1(x) = \operatorname{diag}\{\frac{\bar{q}SC_L + F_T\alpha}{mV}, \left(\frac{\rho VSC_{L\alpha}}{2m} + \frac{F_T}{mV}\right)\}\\ x_{2\mathsf{s}} = [\mu, \alpha]^{\mathsf{T}}.\end{gathered}$$

Using Theorem 1 for our outer-loop control design we determine the desired control sub-vector $x_{2\mathsf{sd}}$ components as follows:

$$\begin{gathered}\mu_{\mathsf{d}} = \frac{mV}{\bar{q}SC_L + F_T\alpha}\left[-\frac{\bar{q}SC_Y}{mV} - k_\chi\hat{\chi} + \dot{\chi}_{\mathsf{d}}\right]\\ \alpha_{\mathsf{d}} = \frac{m}{\frac{\rho VSC_{L\alpha}}{2} + \frac{F_T}{V}}\left[-\frac{\Delta f_\gamma(x)}{m} - k_\gamma\hat{\gamma} + \dot{\gamma}_{\mathsf{d}}\right]\\ \hat{\chi} = (\chi - \chi_{\mathsf{d}}),\ \hat{\gamma} = (\gamma - \gamma_{\mathsf{d}}).\end{gathered}$$

in order to simplify controller design, we recall that $\beta_{\mathsf{d}} = \dot{\beta}_{\mathsf{d}} = 0$, therefore $x_{2\mathsf{d}} = [\mu_{\mathsf{d}}, \alpha_{\mathsf{d}}, 0]^{\mathsf{T}}$. The corresponding error dynamics for x_1 are as follows

$$\dot{\hat{x}}_1 = -\operatorname{diag}\{k_\chi,\ k_\gamma\}\hat{x}_1 + \operatorname{diag}\{G_1(x), 0\}\hat{x}_2.$$

C. Angle of Attack, Slide-slip, and Bank-angle Control

Let $x_2 = [\mu, \alpha, \beta]^{\mathsf{T}}$ be a vector containing the bank-angle μ, angle of attack α, and slide-slip angle β. A differential equation relating $\dot{x}_2$ to x_2 the angular velocity $\omega = x_3$ and force-disturbance vector $\Delta f_{x_2}(x) = [\Delta f_\mu(x), \Delta f_\alpha(x), \Delta f_\beta(x)]^{\mathsf{T}}$ based on (16), (15), and (17) is a follows:

$$\begin{gathered}\dot{x}_2 = F_2(x) + G_2(x)x_3\\ F_2(x) = A_{x_2}(x)x_2 + \Delta f_{x_2}(x)\\ A_{x_2}(x) = -\operatorname{diag}\left\{0, \frac{F_T + \bar{q}SC_{L\alpha}}{mV}, \frac{F_T - \bar{q}S\left(C_{Y\beta} + C_{Ds}\right)}{mV}\right\}\\ G_2(x) = \begin{bmatrix} 1 & 0 & \alpha\\ 0 & \left(1 - \frac{\rho C_{Lq}\bar{c}}{4m}\right) & 0\\ \left(\alpha + \frac{\rho C_{Yp}b}{4m}\right) & 0 & \left(-1 + \frac{\rho C_{Yr}b}{4m}\right)\end{bmatrix}.\end{gathered}$$

Note that $\omega = x_3,\ \omega_{\mathsf{d}} = x_{3\mathsf{d}}$ is now the control input, therefore we implement the following back-stepping controller proposed in Theorem 1:

$$\begin{aligned}\omega_{\mathsf{d}} =& G_2^{-1}(x)[-F_2(x) - k_2\hat{x}_2 + \dot{x}_{2\mathsf{d}}\\ &- \operatorname{diag}\{G_1^{\mathsf{T}}(x), 0\}[\hat{x}_1^{\mathsf{T}}, 0]^{\mathsf{T}}]\end{aligned}.$$

With the following desired trajectory determined for ω the error dynamics for x_2 are as follows:

$$\dot{\hat{x}}_2 = -k_2\hat{x}_2 + G_2(x)\hat{\omega} - \operatorname{diag}\{G_1^{\mathsf{T}}(x), 0\}[\hat{x}_1^{\mathsf{T}}, 0]^{\mathsf{T}}.$$

D. Angular Velocity Control

Using Theorem 1 to guide our control design we design our most inner-loop control law for the angular velocity controller. We note that the angular velocity dynamics from (18) can be expressed as

$$\dot{x}_3 = F_3(x) + G_3(x)u$$

in which $x_3 = \omega$, $F_3(x) = -I^{-1}\omega \times I\omega$, $u = \Gamma_c$ and $G_3(x) = I^{-1}$. Therefore, the following control law is chosen:

$$\begin{gathered}\Gamma_c = -IF_3(x) - k_\omega I\hat{\omega} + I\dot{\omega}_{\mathsf{d}} - IG_2^{\mathsf{T}}(x)\hat{x}_2\\ \Gamma_\delta = \Gamma_c - (\Gamma_\omega + \Gamma_{\mathsf{d}})\\ \delta = \left(\frac{1}{\bar{q}S}\right)\begin{bmatrix} 0 & C_{l\delta_a} & C_{l\delta_r}\\ C_{m\delta_e} & 0 & 0\\ 0 & C_{n\delta_a} & C_{n\delta_r}\end{bmatrix}^{-1}\Gamma_\delta\\ \hat{\omega} = (\omega - \omega_{\mathsf{d}})\end{gathered}$$

This control law results in the following system of equations describing the resulting angular velocity error dynamics

$$\dot{\hat{\omega}} = -k_\omega \hat{\omega} - G_2^{\mathsf{T}}(x)\hat{x}_2.$$

Taking the derivative of the desired trajectory terms $\dot{x}_{j\mathsf{d}}$ can introduce quite a bit of noise and be sensitive to the sampling rate T_s, therefore the trajectory-derivatives are approximated using the following transfer-function and then implemented for the discrete-time case using the *IPESH*-Transform:

$$\dot{x}_{j\mathsf{d}}(s) \approx \text{diag}\left\{\frac{s}{\frac{N_j T_s}{\pi}s + 1}\right\} x_{j\mathsf{d}}(s),\ N_j = 10 \text{ typical.}$$

VI. SIMULATION AND VERIFICATION

In simulating our proposed control law we set $\dot{x}_{2d} = 0$ because we found that cascading three derivative terms related to the desired trajectories was to aggressive a control law to attempt without trying to apply some rate-limiting technique to the system such as those proposed by [17]. All other controllers were implemented as discussed and performed quite satisfactory without little need for control gain tuning. The aircraft we chose to simulate is the Cessna A-37 Dragonfly, a United States Air Force light attack aircraft whose properties are summarized in Table I.

TABLE I

AIRCRAFT MASS, INERTIA, GEOMETRIC, AND DRAG PARAMETERS.

m (kg)	I_{xx} (kg-m^2)	I_{yy} (kg-m^2)	I_{zz} (kg-m^2)	$-I_{xz}$ (kg-m^2)
$2,885$	$10,833$	$4,515$	$15,185$	317
b (m)	$\bar{c}$ (m)	S (m^2)		
10.302	1.667	16.908		
$C_{D\alpha}$	C_{Do}	$C_{D\text{in}}$	C_{Dq}	$C_{D\delta_e}$
0.384	0.048	0	0	0
$C_{L\alpha}$	C_{Lo}	$C_{L\text{in}}$	C_{Lq}	$C_{L\delta_e}$
5.15	0.2	0	4.1	0.5
$C_{Y\beta}$	C_{Yo}	C_{Yp}	C_{Yr}	$(C_{Y\delta_a}, C_{Y\delta_r})$
-0.346	0	-0.0827	0.3	(0, 0.2)
$C_{l\beta}$	C_{lo}	C_{lp}	C_{lr}	$(C_{l\delta_a}, C_{l\delta_r})$
-0.0944	0	-0.442	0.0926	(-0.181, 0.015)
$C_{n\beta}$	C_{no}	C_{np}	C_{nr}	$(C_{n\delta_a}, C_{n\delta_r})$
0.1106	0	-0.0243	-0.139	(0.0254, -0.0365)
$C_{m\alpha}$	C_{mo}	$C_{m\text{in}}$	C_{mq}	$C_{m\delta_e}$
-0.7	0.025	0	-14.9	-1.12

A. Test Flight Conditions

An aggressive flight path is chosen in order to fully verify the effectiveness of our proposed control law and test our fixed-wing aircraft model. The corresponding desired velocity $V_{\mathsf{d}}(t)$, velocity flight-path angle $\gamma_{\mathsf{d}}(t)$ and velocity heading angle $\chi_{\mathsf{d}}(t)$ trajectories are depicted in Fig. 3 and Fig. 4 respectively. All controllers tested used the following gains $k_\chi = 0.5$, $k_\gamma = k_2 = k_3 = 1$. Using the control law proposed in Theorem 1 the resulting aerodynamic angles $x_{2\mathsf{d}}(t)$ and angular velocities $\omega(t)$ are depicted in Fig. 5 and Fig. 6 respectively. Note that the corresponding angle of attack when $\gamma = 0$ corresponds closely to the trim conditions predicted in Section IV and plotted in Fig. 7.

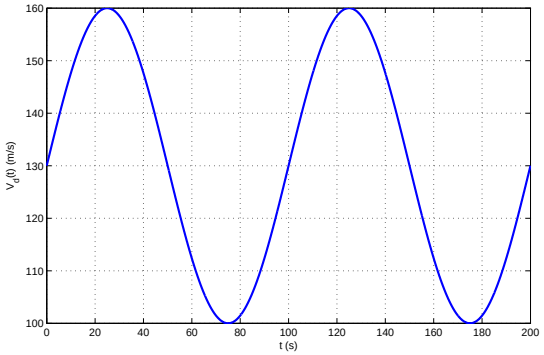

Fig. 3. Desired velocity trajectory $V_{\mathsf{d}}(t)$.

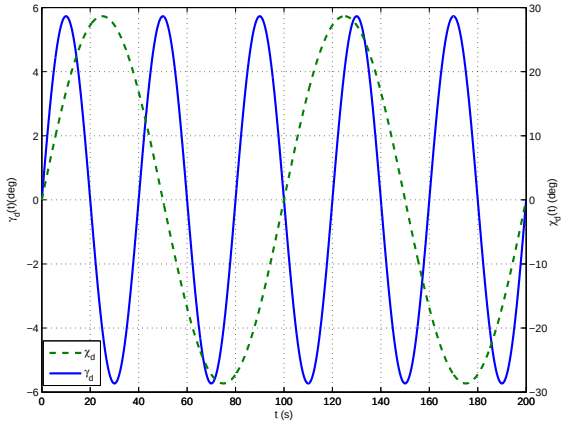

Fig. 4. Desired velocity flight-path angle $\gamma_{\mathsf{d}}(t)$ and velocity heading angle $\chi_{\mathsf{d}}(t)$ trajectories.

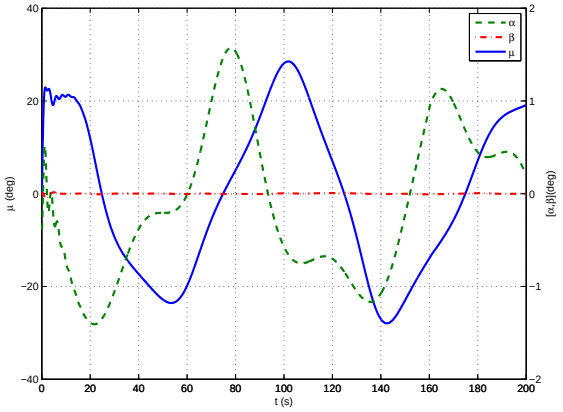

Fig. 5. Resulting $x_2(t)$ to achieve nominal flight trajectories (no wind).

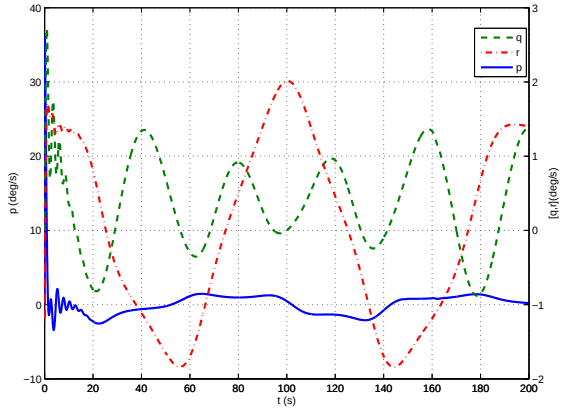

Fig. 6. Resulting $\omega(t)$ to achieve nominal flight trajectories (no wind).

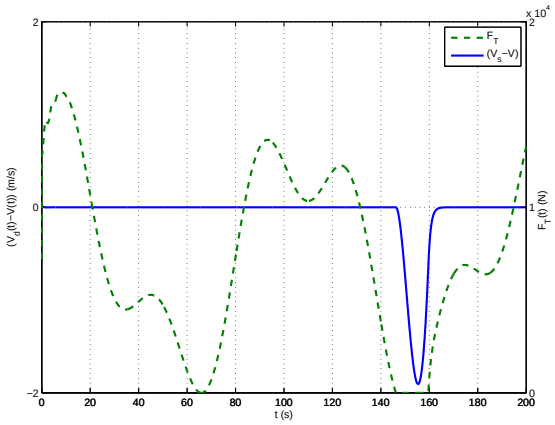

Fig. 8. Nominal velocity tracking error $(V_d(t) - V(t))$ and control thrust $F_T(t)$.

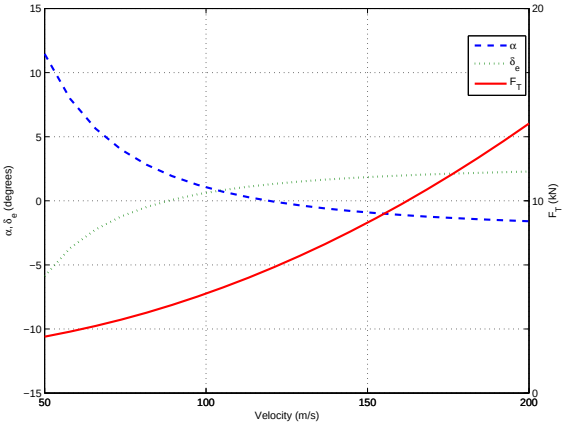

Fig. 7. Trim conditions for Cessna A-37.

B. Controller Tracking Performance

The velocity control system worked with near perfect tracking except when the desired control thrust was less than zero. In order to account for such an unfeasible velocity set-point a classic anti-windup compensation scheme was used to limit the integrator [20]. In particular the control law proposed in Section V-A was modified as follows:

$$
\begin{aligned}
F_{Tp} &= \bar{q}S(C_{\mathsf{Do}} + C_{\mathsf{Din}}\delta_f) - \Delta f_V(x) - m\omega_c V + F_{Tc} \\
F_T &= \mathrm{sat}(F_{Tp}, 0, F_{\max}) \\
\bar{u} &= F_T - F_{Tp} \\
\dot{\bar{V}} &= -\omega_c \bar{V} + \frac{1}{m}\bar{u} \\
\frac{F_{Tc}(s) - mV_{\mathsf{d}}(s)}{V_{\mathsf{d}}(s) - (V(s) + \bar{V}(s))} &= mk_V \frac{s+\omega_c}{s}.
\end{aligned}
$$

The resulting control output F_T and tracking error $V(t) - V_d(t)$ are depicted in Fig. 8. From Fig. 8 it is clear that nearly perfect tracking of $V_{\mathsf{d}}(t)$ is achieved unless actuator saturation occurs, in which the anti-windup control law preserves stability while quickly regaining desired velocity control when saturation is no-longer present. When the aircraft is not subject to either headwind or gust type disturbances, the control system for γ and χ tracks the desired trajectories as depicted in Fig. 9. Similar tracking performance is achieved when the aircraft is subject to a steady wind shear model [21], however, when an additional discrete wind-gust [21] is applied at 100 seconds with a magnitude $[5, 5, 5]$ (m/s) over a distance $10b$ results in significant oscillations which take over twenty seconds to settle. Significantly, better robustness to the discrete wind-gust disturbance is achieved with the less complex controller proposed in Theorem 2 whose error tracking performance is depicted in Fig. 10. The gust disturbance is quite significant as can be seen from the angle-of-attack, slide-slip-angle and bank-angle responses depicted in Fig. 11. The wind gust applied to the aircraft caused the angle-of-attack to drop from $-0.5°$ to $-2.0°$ in less than one second which corresponds to a decrease in the lift force from 25 kN to 5 kN. Although the controller proposed in Theorem 1 has a longer settling time then the less complex controller, the maximum deviation from the desired set-point for γ is less. Such a result suggests that by filtering the additional controller term $-G^{\mathsf{T}}(x)\hat{x}$ could still reduce the tracking error while reducing settling time. In particular we apply the modified control law:

$$
\begin{aligned}
u =& G_m^{-1}(x)(-F_m(x) - k_m\hat{x}_m + \dot{x}_{m\mathsf{d}} - y_{m-1}) \\
\tau_f\dot{y}_{m-1} =& -y_{m-1} + G_{m-1}^{\mathsf{T}}(x)\hat{x}_{m-1} \\
x_{m\mathsf{d}} =& G_{m-1}^{-1}(x)(-F_{m-1}(x) - k_{m-1}\hat{x}_{m-1} + \dot{x}_{(m-1)\mathsf{d}} \\
=& \quad -y_{m-2}) \\
\tau_f\dot{y}_{m-2} =& -y_{m-2} + G_{m-2}^{\mathsf{T}}(x)\hat{x}_{m-2} \\
\vdots =& \quad \vdots \\
x_{3\mathsf{d}} =& G_2^{-1}(x)\left(-F_2(x) - k_2\hat{x}_2 + \dot{x}_{2\mathsf{d}} - y_1\right) \\
\tau_f\dot{y}_1 =& -y_1 + G_1^{\mathsf{T}}(x)\hat{x}_1 \\
x_{2\mathsf{d}} =& G_1^{-1}(x)\left(-F_1(x) - k_1\hat{x}_1 + \dot{x}_{1\mathsf{d}}\right)
\end{aligned}
$$

which achieves improved disturbance rejection and tracking as can be seen in Fig. 12 and reduces the deviation in angle-of-attack as seen in Fig. 11 which reduces the overall force-deviation applied to the aircraft. Finally Fig. 14 indicates

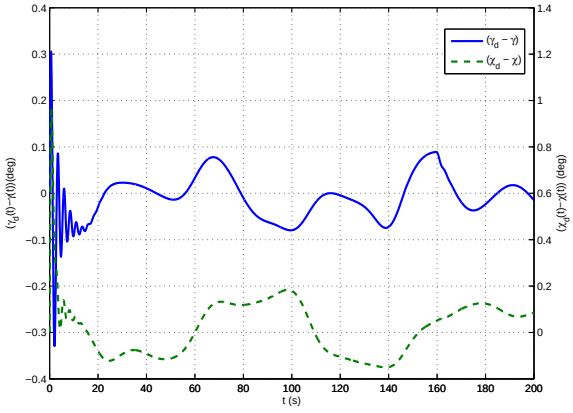

Fig. 9. Nominal flight-path angle γ and velocity heading angle χ tracking error.

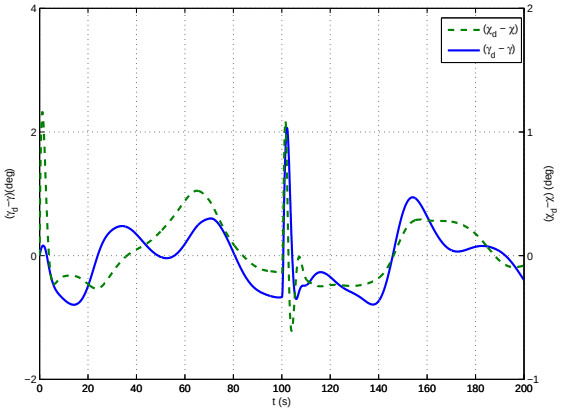

Fig. 10. Flight-path angle γ and velocity heading angle χ tracking error when subject to steady wind shear and a gust at 100 s using control law from Theorem 2).

that the velocity controller works exceptionally well in maintaining desired velocity in spite a significant wind gust disturbance.

VII. CONCLUSIONS

We have presented a simplified back-stepping control law which does not use adaptation in order to verify fixed-wing aircraft models. In doing show we showed that this control law is quite robust to controlling the aircraft in both steady winds and significant discrete wind-gusts. In addition, the controller performs exceptionally well as compared to more complex adaptive back-stepping controllers. In particular, assuming a small angle assumption on α, β and μ, greatly simplifies the control laws while still getting similar range and performance as compared to the controller implemented in [10]. Careful inspection of the proof for Theorem 1, for example will show that although back-stepping controllers can invert functions such at $\tan(x)$ which may be embedded in the $G(x)$ description do not necessarily lead to perfect cancellation of their effects which result in the idealized negative definite Lyapunov functions presented. However,

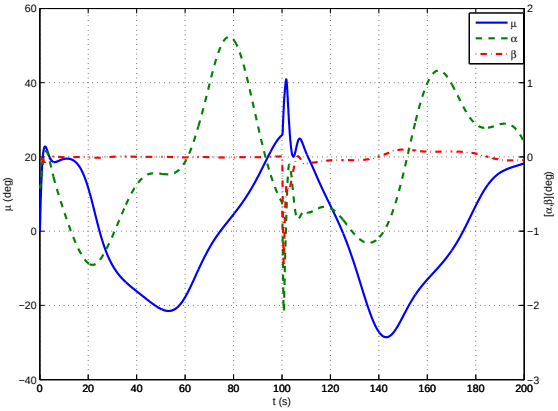

Fig. 11. Resulting $x_2(t)$ to achieve flight trajectories when subject to steady wind shear and a gust at 100 s using control law from Theorem 2).

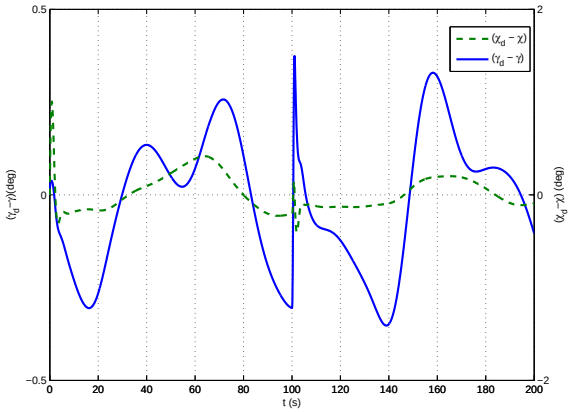

Fig. 12. Flight-path angle γ and velocity heading angle χ tracking error when subject to steady wind shear and a gust at 100 s using improved control law.

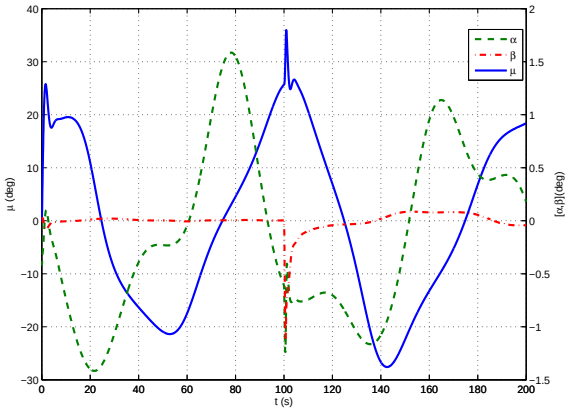

Fig. 13. Resulting $x_2(t)$ to achieve flight trajectories when subject to steady wind shear and a gust at 100 s using improved control law.

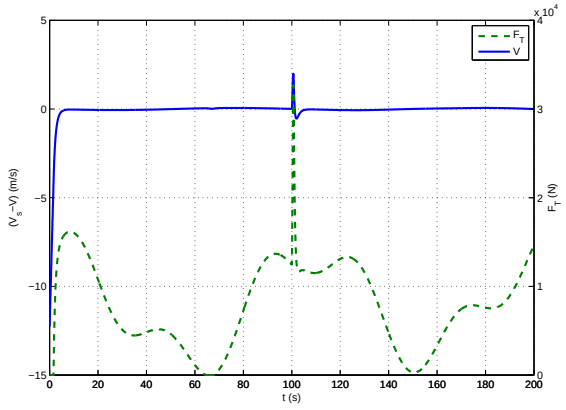

Fig. 14. Resulting $\hat{V}$ and F_T to achieve velocity trajectory when subject to steady wind shear and a gust at 100 s.

arguments similar to those given in Theorem 2 are sufficient to state that if the gains are large enough these non-ideal effects are typically compensated sufficiently to maintain a negative definite function. Theorem 2 led to a more robust controller which led us to propose a filtered version of Theorem 1 which resulted in our best controller as presented in Section VI-B.

REFERENCES

[1] P. Castillo, A. Dzul, and R. Lozano, "Real-time stabilization and tracking of a four-rotor mini rotorcraft," *Control Systems Technology, IEEE Transactions on*, vol. 12, no. 4, pp. 510–516, 2004.

[2] A. Teel, "Global stabilization and restricted tracking for multiple integrators with bounded controls," *Systems & Control Letters*, vol. 18, no. 3, pp. 165–171, 1992.

[3] ——, "A nonlinear small gain theorem for the analysis of control systemswith saturation," *Automatic Control, IEEE Transactions on*, vol. 41, no. 9, pp. 1256–1270, 1996.

[4] A. Tayebi and S. McGilvray, "Attitude stabilization of a VTOL quadrotor aircraft," *Control Systems Technology, IEEE Transactions on*, vol. 14, no. 3, pp. 562–571, 2006.

[5] T. Hamel and R. Mahony, "Image based visual servo control for a class of aerial robotic systems," *Automatica*, vol. 43, no. 11, pp. 1975–1983, 2007.

[6] N. Kottenstette and J. Porter, "Digital passive attitude and altitude control schemes for quadrotor aircraft," Institute for Software Integrated Systems, Vanderbilt University, Nashville, TN, Tech. Rep. ISIS-08-911, 11 2008, to Appear ICCA 2009.

[7] G. M. Hoffmann, H. Huang, S. L. Waslander, and C. J. Tomlin, "Quadrotor helicopter flight dynamics and control: Theory and experiment," *Collection of Technical Papers - AIAA Guidance, Navigation, and Control Conference 2007*, vol. 2, pp. 1670 – 1689, 2007.

[8] M. Krstic, P. Kokotovic, and I. Kanellakopoulos, *Nonlinear and adaptive control design*. John Wiley & Sons, Inc. New York, NY, USA, 1995.

[9] O. Härkegård, "Backstepping and control allocation with applications to flight control," Ph.D. dissertation, Linköping University, 2003.

[10] J. Farrell, M. Sharma, and M. Polycarpou, "Backstepping-based flight control with adaptive function approximation," *Journal of Guidance, Control, and Dynamics*, vol. 28, no. 6, pp. 1089–1102, 2005.

[11] J. Diebel, "Representing Attitude: Euler Angles, Unit Quaternions, and Rotation Vectors," Technical report, Stanford University, California, USA, Tech. Rep., 2006.

[12] L. Mangiacasale, *Flight Mechanics of a [mu]-airplane: With a Matlab Simulink Helper*. Edizioni Libreria CLUP, 1998.

[13] B. L. Stevens and F. L. Lewis, *Aircraft Control and Simulation*, 2nd ed. John Wiley & Sons, Inc., 2003.

[14] G. Campa, Y. Gu, B. Seanor, M. Napolitano, L. Pollini, and M. Fravolini, "Design and flight-testing of non-linear formation control laws," *Control Engineering Practice*, vol. 15, no. 9, pp. 1077–1092, 2007.

[15] M. S. Selig, R. Deters, and G. Dimock, "Aircraft dynamic models for use with flightgear," *Aircraft-uiuc*, p. 5, 2002. [Online]. Available: http://www.ae.illinois.edu/m-selig/apasim/Aircraft-uiuc.html

[16] Y. Zou, P. Pagilla, and R. Ratliff, "Distributed Formation Flight Control Using Constraint Forces," *JOURNAL OF GUIDANCE, CONTROL, AND DYNAMICS*, vol. 32, no. 1, 2009.

[17] J. Farrell, M. Polycarpou, and M. Sharma, "On-line approximation based control of uncertain nonlinear systems with magnitude, rate and bandwidth constraints on the states and actuators," *Proceedings of the 2004 American Control Conference*, pp. 2557–2562, 2004.

[18] N. Kottenstette, J. Hall, X. Koutsoukos, P. Antsaklis, and J. Sztipanovits, "Digital control of multiple discrete passive plants over networks," *International Journal of Systems, Control and Communications (IJSCC)*, no. Special Issue on Progress in Networked Control Systems, 2009, to Appear.

[19] N. Kottenstette, H. LeBlanc, E. Eyisi, and X. Koutsoukos, "Multi-rate networked control of conic systems," Institute for Software Integrated Systems, Vanderbilt University, Nashville, TN, Tech. Rep., 09/2009 2009.

[20] Y. Fu, N. Kottenstette, Y. Chen, C. Lu, X. Koutsoukos, and H. Wang, "Feedback thermal control for real-time systems," Washington University in St. Louis, St. Louis, MO, Technical Report, 06/2009 2009, to Appear RTAS 2010, Stockholm, Sweden.

[21] D. Moorhouse and R. Woodcock, "US Military Specification MIL–F–8785C," Technical report. US Department of Defense, Tech. Rep., 1980.